Tunneling Resonances and Coherence in an Optical Lattice

B. K. Teo, J. R. Guest, and G. Raithel

FOCUS Center, Physics Department, University of Michigan, 500 East University, Ann Arbor, Michigan 48109-1120

(Received 9 August 2001; published 10 April 2002)

The center-of-mass quantization of atoms trapped in a gray optical lattice is observed to manifest itself in the steady-state properties of the atoms. Modulations in the lifetime and macroscopic magnetization as a function of an applied **B** field are attributed to quantum mechanical tunneling resonances and are shown to exist only under conditions which afford spatial coherence of the trapped atoms over several lattice wells and coherence times that exceed the tunneling period.

DOI: 10.1103/PhysRevLett.88.173001 PACS numbers: 32.80.Pj, 03.65.Xp, 32.80.Lg

Optical lattices, which are periodic arrays of light-shift potential wells used to cool and localize atoms [1], have offered insight into quantum dynamics and have been proposed as platforms for quantum computing [2]. The quantum nature of the center-of-mass motion (c.m.) of the trapped atoms has been found to manifest itself in transient phenomena such as Landau-Zener tunneling [3], Bloch oscillations [4], Wannier-Stark states [5], wave-packet revivals [6], and tunneling [7–9]. In this paper, we demonstrate that the c.m. quantization can be observed not only in (time-dependent) wave-packet experiments, but also in the *steady-state* properties of trapped atoms, as has been predicted previously [10]. We use an external magnetic field **B** to induce observable **B**-dependent variations in the lifetime and the steady-state magnetization of the entire atomic sample, which we attribute to c.m. quantization and well-to-well tunneling. The phenomena open up novel opportunities for the preparation of cold atoms and the assessment of quantum coherence in optical lattices.

Our theoretical studies reveal an intimate relation between the steady-state manifestations of the c.m. quantization and the coherence properties of the trapped atoms. We find that the visibility of the modulations in the steady-state magnetization acts as a sensitive probe for long coherence times and spatial well-to-well coherence of the trapped atom wave functions.

Our 1D gray lattice [11,12] is formed by two counterpropagating laser beams with mutually orthogonal linear polarizations [1]. The lattice light is blue-detuned by 6Γ from the $F = 2 \rightarrow F' = 2$ transition of the ^{87}Rb D1 line ($\Gamma = 6$ MHz $\times 2\pi$, $\lambda = 795$ nm) and has a single-beam intensity of $I = 6.3$ mW/cm^2. Atoms lost into the $F = 1$ hyperfine level of the ground state are repumped into the optical lattice by a weak repumper laser tuned to the D2 $F = 1 \rightarrow F' = 2$ transition. The atoms are laser cooled into the lowest adiabatic light-shift potential (LAP) of the optical lattice, which is well separated from the other higher-lying adiabatic potentials. Because of the presence of another excited hyperfine level ($F' = 1$) and a gauge potential [7,13], the LAP exhibits a modulation of order $10E_R$ [the recoil energy $E_R = \hbar^2 k_L^2/(2M)$ with $k_L = 2\pi/\lambda$]. The minima of the LAP are exactly zero and coincide with the locations of pure σ^+ and σ^- light polarizations; the latter occur in alternating order and are separated by $\lambda/4$. The σ^+ and σ^- wells are populated by atoms in spin states $|m_F = +2\rangle$ and $|m_F = -2\rangle$, respectively. Quantum mechanically, the LAP supports a few tightly bound bands in which the cooled atoms accumulate. The fluorescence-induced decay rates in these bands are exceptionally low, leading to steady-state temperatures near the recoil limit and long quantum coherence times; the latter property of the gray optical lattice is critical for our observations.

If there is no external magnetic field **B** applied to the lattice, the σ^+ and σ^- wells are symmetric, and the atoms are equally distributed between them. Because of the Zeeman effect, a **B**-field parallel to the lattice quantization axis (longitudinal field $B_\parallel$) raises and lowers the σ^+ and σ^- wells, respectively [14]. The atoms preferentially populate the deeper wells and therefore a steady-state magnetization of the entire atomic sample develops [14,15]. However, at certain values of $B_\parallel$ the states in the upshifting and downshifting wells are tuned into resonance with one another; this leads to well-to-well tunneling which drastically alters the quantum dynamics of the system. At these values, we observe modulations of the magnetization and lifetime of the trapped atoms.

The experiment is conducted in a vapor-cell magneto-optical trap (MOT). During the first 14 ms of each 16.6 ms experimental cycle, the MOT collects and cools of order 10^7 atoms. After turning off the MOT magnetic field, the atoms are further cooled for 1 ms in a 3D optical molasses. The atoms are then loaded into our gray 1D optical lattice. Three orthogonal pairs of Helmholtz coils are used to cancel the background magnetic field to below 1 mG and to apply a controlled magnetic field. The gray lattice cools the atoms for 1.6 ms into the lowest bands of the LAP.

At the end of the lattice cooling phase, the magnetization of the sample is determined by measuring the transmission of a weak probe beam tuned to the D2 $F = 2 \rightarrow F' = 3$ transition for both circular polarizations. For the predominantly populated substates $|m_F = \pm 2\rangle$, the squares of the Clebsch-Gordon coefficients for the absorption of

σ^+ and σ^- light differ by a factor of 15. The measured transmission factors for σ^+ and σ^- light are denoted by t_+ and t_-, respectively, and n_+ and n_- denote the respective area densities of the atoms in the states $|m_F = +2\rangle$ and $|m_F = -2\rangle$. For probe intensities well below the saturation intensity, sufficiently short probe pulses, probe beam diameters smaller than the atomic cloud, and under the valid approximation that all atoms are in one of the states $|m_F = \pm 2\rangle$, the area densities can be obtained from

$$n_{+(-)} = -\frac{2I_{\text{sat}}\lambda}{\Gamma hc}\left\{\ln(t_{+(-)}) - \frac{1}{15}\ln(t_{-(+)})\right\}, \quad (1)$$

where the saturation intensity $I_{\text{sat}} = 1.6\ \text{mW/cm}^2$. We can then ascertain the average magnetization $\langle m_F\rangle = F\{n_+ - n_-\}/\{n_+ + n_-\}$ and the total area density $n_{\text{tot}} = n_+ + n_-$.

In Fig. 1a, the steady-state magnetization $\langle m_F\rangle$ and the area density n_{tot} are shown as a function of $B_\parallel$. The curve $\langle m_F\rangle(B_\parallel)$ exhibits an overall paramagnetic behavior, as expected [10], and about six modulations with a periodicity of $\sim$10 mG. As explained below, the modulations are caused by tunneling resonances between the σ^+ and σ^- wells of the LAP. The modulations do not persist above $|B_\parallel| \approx 30$ mG because one type of well ceases to support bound states. The weak variation of n_{tot} is merely due to the $B_\parallel$ dependence of the MOT performance.

The paramagnetism and the modulations of the magnetization curves are reproduced by our quantum Monte Carlo wave function simulations (QMCWS) [16] (thick line in Fig. 1a). The simulations have also confirmed that the applied cooling time of 1.6 ms is long enough for the atoms to reach their steady-state magnetization. The simulations generally predict absolute magnetization values that are about 40% larger than the values observed in the experiment, and the modulations obtained in the simulations are more pronounced. This quantitative disparity can be explained by time-dependent environmental magnetic fields and imperfections in the lattice and repumper laser beam profiles and polarizations.

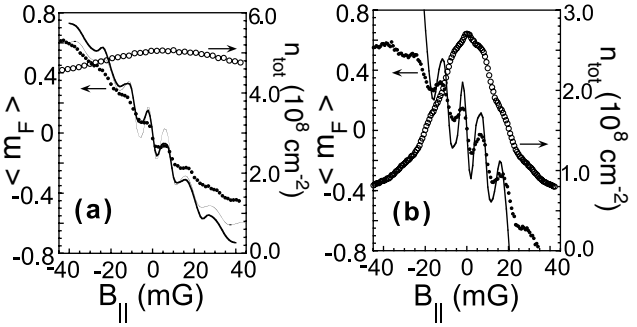

FIG. 1. Magnetization $\langle m_F\rangle$ (dots) and area density n_{tot} (open circles) of a gray optical lattice as a function of $B_\parallel$, measured (a) in steady state and (b) after evolution without the repumper for 600 μs. The thick lines are results of QMCWS. The thin line in (a) shows the result from a band-structure-based model (discussed later).

The repumping light plays a much larger role in our gray lattice than in bright optical lattices or molasses. Since we operate near an $F = 2 \rightarrow F' = 2$ transition, in about 50% of the events in which an atom scatters a lattice photon, the atom decays into the $F = 1$ level of the ground state and subsequently absorbs a repumper photon. Therefore, the radiation pressure and the polarization of the repumper laser have a significant influence on the cooling performance and the average magnetization of the trapped atoms [17]. Taking advantage of these repumping properties, we can selectively remove atoms with high photon scattering rates through optical pumping into the $F = 1$ level by turning off the repumper laser. Atoms in the higher bands of the lattice scatter many more photons than atoms cooled into the lowest few bands and will therefore be much more susceptible to the optical pumping. The coldest atoms, which include those producing the modulations in $\langle m_F\rangle(B_\parallel)$, are retained in the lattice. Since we measure the magnetization of only the atoms left in the lattice, the significance of the modulations in $\langle m_F\rangle(B_\parallel)$ is enhanced. Further, the technique allows us to obtain information on the typical lifetime of the Bloch states in which the atoms are trapped.

In Fig. 1b, we show the magnetization and area density for the same parameters as in Fig. 1a, except that during the last 600 μs of the 1.6 ms cooling time the repumper laser is turned off. Clearly, the selective removal of the atoms with above-average energies greatly enhances the modulations in the magnetization of the atoms in the lattice. We compare the experimental result with QMCWS and find good qualitative agreement. The bell-shaped curve $n_{\text{tot}}(B_\parallel)$ in Fig. 1b shows that generally low photon scattering rates (i.e., long lifetimes of the trapped atoms) can be achieved only for $B_\parallel \lesssim 10$ mG. Further, the curve $n_{\text{tot}}(B_\parallel)$ exhibits modulation structures that coincide with the structures observed in the magnetization curve $\langle m_F\rangle(B_\parallel)$, indicating that the modulations in $\langle m_F\rangle(B_\parallel)$ are related to the behavior of the lifetime of the trapped atoms.

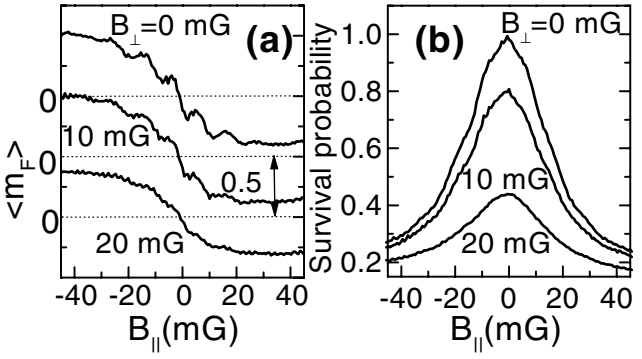

FIG. 2. (a) Average magnetization $\langle m_F\rangle$ of atoms in the lattice as a function of $B_\parallel$ for the indicated values of $B_\perp$, measured after 1 ms of cooling in the lattice and 600 μs evolution without repumper laser. For clarity, the curves are offset from each other. (b) Corresponding survival probabilities of the atoms in the lattice during the repumper-free evolution.

In Fig. 2, it is observed that weak transverse magnetic fields $B_\perp$ do not significantly shift the modulations in $\langle m_F \rangle (B_\parallel)$. This observation is in accordance with tunneling resonances causing the modulations, because small transverse magnetic fields do not significantly alter the LAP and its tunneling resonances.

When a transverse field $B_\perp$ is applied to the lattice, the atomic states associated with the LAP acquire admixtures of $|m_F = \pm 1\rangle$ that lead to an increase of the photon scattering rate and therefore to a reduction of the lifetime of the trapped atoms. This leads to an overall decrease of the survival probability curves in Fig. 2b with $B_\perp$. Comparing Figs. 2a and 2b, it further becomes evident that a high visibility of the modulations requires a long lifetime of the trapped atoms.

In a band-structure-based model (BSBM) of the steady state of the laser cooling process in gray lattices, the population of the bands is proportional to the band-averaged inverse decay rates of the respective Bloch states [18,19]. Since the decay rates generally increase with the band index, the BSBM predicts that atoms accumulate in the lowest bands. Laser cooling and paramagnetism in gray lattices thus follow from the BSBM. Tunneling resonances modify the paramagnetic behavior, as explained in the following for the case of the tunneling resonance between the first excited state in the σ^- wells and the ground state in the σ^+ wells. In our lattice, this resonance is centered at $B_\parallel = 10$ mG. In Fig. 3, we show the band structure and the decay rates of the Bloch states for the lowest three bands at a slightly smaller field, $B_\parallel = 8$ mG, and at a slightly larger field, $B_\parallel = 12$ mG. At $B_\parallel = 8$ mG, the second band consists of Bloch states that are primarily associated with the ground state in the upshifting wells. The anomalously low decay rates in the second band lead to unusually large populations in the upshifting wells. Thus, at $B_\parallel = 8$ mG the usual paramagnetic behavior of the lattice is suppressed. Above the tunneling resonance (12 mG), the band-averaged decay rates follow the usual pattern, i.e., they increase with the band index. Therefore, in the vicinity of the tunneling resonance the magnetic behavior switches from weakly to quite strongly paramagnetic, resulting in an exceptionally large slope of the magnetization curve $\langle m_F \rangle (B_\parallel)$ at $B_\parallel \approx 10$ mG. An analogous behavior is observed at all tunneling resonances. We find excellent agreement between the experimental values of $B_\parallel$ where extrema of $d\langle m_F \rangle / dB_\parallel$ occur and the values of $B_\parallel$ at which theory predicts tunneling resonances.

Further insight is obtained by a quantitative analysis of some results of the BSBM of the steady-state lattice. The populations of the Bloch states are inversely proportional to their decay rates $\gamma(n, q)$, and the average magnetization is $\langle m_F \rangle = \{\sum_{n,q} \bar{m}(n, q)\gamma(n, q)^{-1}\}/\{\sum_{n,q} \gamma(n, q)^{-1}\}$, where n is the band index, q the quasimomentum, and $\hbar\bar{m}(n, q)$ the expectation value of the z component of $\hat{\mathbf{F}}$ of the Bloch state (n, q). In Fig. 1a, the BSBM (thin line) agrees well with our other findings. A contour plot of $\langle m_F \rangle (B_\parallel, B_\perp)$ shown in Fig. 4 demonstrates that the BSBM reproduces the tunneling-induced modulations of the magnetization. The shaded region indicates the field range in which the averaged lifetime $\langle \tau \rangle = \{\sum_{n,q} \gamma(n, q)^{-2}\}/\{\sum_{n,q} \gamma(n, q)^{-1}\} > 100$ μs. Noting that the tunneling period is ≈ 150 μs [7] and that the modulations are only prominent inside the shaded region, we conclude that the average lifetime $\langle \tau \rangle$ must be comparable with or larger than the tunneling period for the magnetization modulations to become clearly observable.

We now discuss the implications of these findings for the coherence properties of the trapped atoms. Analyzing the Bloch functions, we found that the lifetime variations

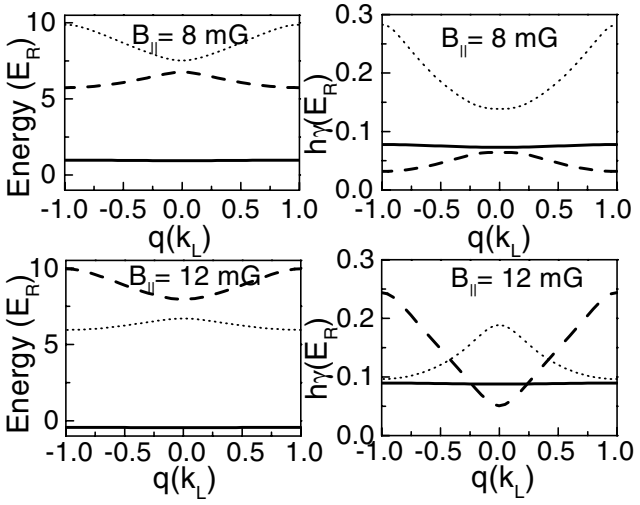

FIG. 3. Real (left) and imaginary (right) parts of the band energies vs quasimomentum q for $B_\parallel = 8$ mG (upper) and $B_\parallel = 12$ mG (lower) for our optical lattice. The solid (dotted) lines correspond to the lowest (first excited) states of the c.m. motion in the downshifting wells, the dashed lines to the lowest states in the upshifting wells.

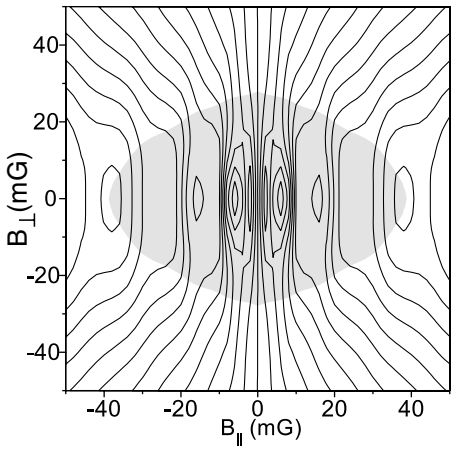

FIG. 4. Contour lines of $\langle m_F \rangle$ obtained from the band-structure-based model. The separation between adjacent lines is 0.05. In the shaded field range, the average lifetime $\langle \tau \rangle$ exceeds 100 μs.

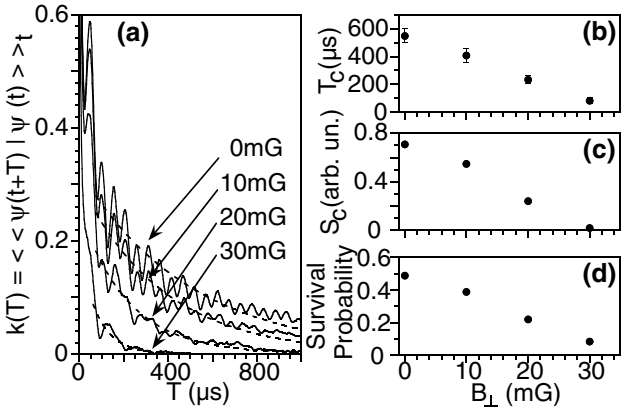

FIG. 5. QMCWS results. (a) Steady-state autocorrelation functions $k(T)$ for $B_\parallel = 0$ and $B_\perp = 0$, 10, 20, and 30 mG. The oscillations in the $k(T)$ reflect random-phase wave-packet and tunneling oscillations. The dashed lines are decaying exponential fits to $k(T)$. The $B_\perp$ dependence of the coherence decay time T_c and the spatial well-to-well coherence parameter S_c are shown in (b) and (c), respectively. For comparison, we show in (d) the probability that an atom remains in the lattice over a period of 600 μs without the repumper laser.

exist because the admixture of $5P_{1/2}$ character to the Bloch states is—depending on the exact value of $B_\parallel$—enhanced or suppressed by constructive or destructive interference of excitation pathways. Since the lattice light contains only σ^+ and σ^- components, each $5P_{1/2}$ magnetic sublevel $|F' = 2, m_F'\rangle$ has (at most) two excitation pathways, namely excitation from the $5S_{1/2}$ sublevels $|F = 2, m_F' \pm 1\rangle$. The interference of these excitation pathways hinges on the local coherence of the Bloch wave functions in the spin degree of freedom. The fact that the interference manifests itself in observable modulations in $\langle m_F\rangle(B_\parallel)$ shows that the spin coherence of the Bloch states (partially) carries over to the steady-state density matrix of the atoms trapped in the lattice.

Using "quantum trajectories" $|\psi(t)\rangle$ generated by QMCWS, we have also studied the temporal and the spatial coherence of the trapped atoms. We determine the steady-state autocorrelation function, $k(T) = |\langle\langle\psi(t + T)|\psi(t)\rangle\rangle_t|$, and a steady-state well-to-well spatial coherence parameter, $S_c = |\langle\psi(x_0, m_F = -2, t)\psi^*(x_0 + \lambda/4, m_F = +2, t)\rangle_t|$. There, the $\langle\,\rangle_t$ denote averages over t, and x_0 is the location of a σ^--well ($x_0 + \lambda/4$ is the location of a σ^+-well). The expression for $k(T)$ contains the wave function in representation-free form, while the expression for S_c is written in position and m-representation. As shown in Fig. 5a, the curves $k(T)$ approximately follow overall decays $\propto \exp(-T/T_c)$ (dashed lines) with quantum coherence times T_c, which reflect the coherence loss due to photon scattering. Considering the dependence of the T_c and S_c on $B_\perp$ (Figs. 5b and 5c) as well as our earlier findings in Figs. 2 and 4, we conclude that high visibility of the modulations in $\langle m_F\rangle$, long lifetimes, long coherence times, and spatial well-to-well coherence of the trapped atoms are synonymous in our system.

We have observed tunneling-induced modulations in the steady-state magnetization and in the lifetime of atoms trapped in an optical lattice. The visibility of these modulations sheds light on the steady-state coherence properties of the trapped atoms. Theoretical data (not presented) have shown that gray lattices on the ^{87}Rb D2 line and on the ^{85}Rb D1 or D2 lines exhibit similar phenomena. We expect that our results generalize to other atomic species and to 3D gray lattices. In theory and in a few experiments, we have observed that the suppression of the paramagnetic behavior can be sufficiently pronounced so as to produce slightly anti-paramagnetic alignment at the first minimum of the magnetization ($B_\parallel \approx 8$ mG for the lattice discussed). Thus, gray lattices may be used to cool atoms preferentially into low-field-seeking magnetic states, which are frequently used in magnetic atom trapping.

We acknowledge support by the NSF (Grants No. PHY-9875553 and No. PHY-0114336) and partial support by the Chemical Sciences, Geosciences and Biosciences Division of the Office of Basic Energy Sciences, Office of Science, U.S. Department of Energy.

[1] P. S. Jessen and I. H. Deutsch, Adv. At. Mol. Opt. Phys. **37**, 95 (1996).
[2] G. K. Brennen *et al.,* Phys. Rev. Lett. **82**, 1060 (1999); D. Jaksch *et al.,* Phys. Rev. Lett. **82**, 1975 (1999).
[3] Q. Niu *et al.,* Phys. Rev. Lett. **76**, 4504 (1996).
[4] M. BenDahan *et al.,* Phys. Rev. Lett. **76**, 4508 (1996).
[5] S. R. Wilkinson *et al.,* Phys. Rev. Lett. **76**, 4512 (1996).
[6] G. Raithel, W. D. Phillips, and S. L. Rolston, Phys. Rev. Lett. **81**, 3615 (1998).
[7] S. K. Dutta, B. K. Teo, and G. Raithel, Phys. Rev. Lett. **83**, 1934 (1999).
[8] D. L. Haycock *et al.,* Phys. Rev. Lett. **85**, 3365 (2000).
[9] S. K. Dutta and G. Raithel, J. Opt. B **2**, 651 (2000).
[10] K. I. Petsas, J.-Y. Courtois, and G. Grynberg, Phys. Rev. A **53**, 2533 (1996).
[11] J. Guo and P. R. Berman, Phys. Rev. A **48**, 3225 (1993); A. Hemmerich *et al.,* Phys. Rev. Lett. **75**, 37 (1995).
[12] G. Grynberg and J.-Y. Courtois, Europhys. Lett. **27**, 41 (1994).
[13] R. Dum and M. Olshanii, Phys. Rev. Lett. **76**, 1788 (1996).
[14] D. R. Meacher *et al.,* Phys. Rev. Lett. **74**, 1958 (1995); G. Raithel, W. D. Phillips, and S. L. Rolston, Phys. Rev. A **58**, R2660 (1998).
[15] C. Triché *et al.,* Opt. Commun. **126**, 49 (1996).
[16] J. Dalibard, Y. Castin, and K. Mølmer, Phys. Rev. Lett. **68**, 580 (1992); K. Mølmer, Y. Castin, and J. Dalibard, J. Opt. Soc. Am. B **10**, 524 (1993).
[17] S. K. Dutta, N. V. Morrow, and G. Raithel, Phys. Rev. A **62**, 035401 (2000).
[18] Y. Castin and J. Dalibard, Europhys. Lett. **14**, 761 (1991).
[19] In gray lattices, the atomic states are not strongly localized and there is no significant Lamb-Dicke reduction of the decay rates of the low-lying levels.